Inflow effects on tonal noise of axial fan under system resistances

Minjun Park[a], Duck-Joo Lee[a], Hakjin Lee[b]*

[a] Department of Aerospace Engineering, Korea Advanced Institute of Science and Technology (KAIST), Daejeon, 34141, South Korea

[b] School of Mechanical and Aerospace Engineering, Gyeongsang National University, Jinju, Gyeongnam, 52828, South Korea

*Corresponding author e-mail address: hlee@gnu.ac.kr

Abstract

An axial fan operates under system resistances owing to neighboring structures located in the front and back of the fan in the actual operating environment. In particular, the acoustic characteristics of the fan change depending on whether the upstream structures exist since they significantly affect the inflow distribution and inlet pressure. In this study, the measurements on three different shrouded fan configurations are conducted to investigate the inflow effects caused by the existence of the upstream structures on tonal noise radiated from the axial fans. An acoustic fan tester installed in an anechoic chamber facility is designed to simultaneously measure the performance and sound pressure levels of the shrouded fan configurations. In addition, the static pressure correction method is proposed to adjust for changing system resistance owing to the upstream structures. Noise levels radiated from both shrouded fan and shrouded fan with upstream structures are compared under the same system resistance conditions. The influences of upstream structures on discrete tonal noise are discussed in detail. Results show that the tonal noise levels associated with 1st to 4th BPF components of the shrouded fan with the upstream structures increase for all the operating conditions except for the high resistance conditions where the blade stall occurs.

Keywords: Axial fan, Inflow effect, Tonal noise, Acoustic fan tester, System resistance

1. Introduction

Conventional automobiles require an axial fan to cool internal heat sources from a combustion engine and operating air conditioning [1]. Electric vehicles are not exempted because they also have internal heat sources for battery packs and electric motor devices [2]. However, fan noise is one of the principal noise sources [3], even though a cooling fan is an essential component of the mobility of vehicles [4]. The operating environment of the cooling fan depends on the vehicle speed. Consequently, the performance and noise of the fan depend on the operating environment [5, 6]. In the actual operating environment of an automotive cooling fan in an engine room, the grille and front fascia are followed by the condenser and radiator in front of the fan, and the engine blocks are located directly behind the cooling fan as shown in Fig. 1 [7]. However, noise measurement in the free field is unsuitable for representing the operational environment of the fan between upstream and downstream structures [8]. Thus, there is a significant difference in the noise level measured between free field conditions and the actual operating environment, including the inflow effects caused by upstream structures [9].

The most common and identifiable noise emitted from the rotating fan blade can be broadly classified into tonal and broadband components. Tonal noise is generated due to the passage of air over the blade, the aerodynamic force exerted on the fluid by the blade surface and blade-vortex interaction. Tonal noise is the dominant contribution to the overall noise level of the fan because it has high acoustic amplitudes at the blade passing frequency (BPF) and its associated harmonics. Broadband noise results from turbulent flow over the blade, which has non-deterministic and non-periodic acoustic signals. Tonal noise has a much higher acoustic amplitude than broadband noise at a relatively low-frequency range. The low-frequency acoustic signals tend to be judged as more annoying than high frequency and are more difficult to be attenuated. Thus, reducing tonal noise makes a significant contribution to the low-noise axial fan system design.

The acoustic characteristics of the fan under the actual operating environment change due to the existence of the upstream structures, such as a radiator and a condenser, since they significantly affect the inflow distribution, inlet pressure, and system resistance. Many researchers have attempted to measure fan noise at system resistances similar to the real environment [10−15]. In particular, the noise characteristics of the fan under high system resistance conditions have been experimentally investigated [16−20]. Lin et al. [21] experimentally studied the noise characteristics of the cooling fan affected by upstream structures, such as a flat plate. Suzuki et al. [22] investigated the tonal noise associated with the BPFs of an automotive cooling fan, depending on simple upstream and downstream structures. Gérard et al. [23, 24] calculated the unsteady lift generated by the interaction between a rotor and upstream structures and then investigated the acoustic performance of the fan using flow control obstructions. Sturm and Carolus [25] pointed out that the interaction between non-homogeneous flow at the inlet and the rotating blades causes periodic force fluctuations and BPF-related tonal noise. Rynell et al. [26, 27] investigated acoustic installation effects originating from a shrouded fan and an upstream radiator. Pérot et al. [28] demonstrated that the tonal noise of the cooling fan increases owing to the inflow effect caused by the upstream structures through the numerical simulation. Park et al. [29] showed that the tonal prediction of rotor blades should include upstream and downstream structures because the geometry directly affects the tonal noise characteristics.

As aforementioned, inflow velocity and pressure are changed if the upstream structures, such as a radiator or a condenser, are located in front of the axial fan. It causes the axial fan to operate at different system resistances, even though the rotating speed of the fan is set to be the same. In this study, the measurements on three different shrouded fan configurations were conducted to investigate the inflow effects caused by the existence of the upstream structures on tonal noise radiated from the axial fans. An acoustic fan tester installed in an anechoic chamber facility was designed to measure the performance and sound pressure levels (SPLs) of the shrouded fan configurations under various system resistances. In addition, the static pressure correction method was proposed to adjust for the changing system resistance owing to the upstream structures. This correction method is important to investigate the inflow effects so that the intensity and spectral characteristics of the radiated tonal noise technologies can be compared at the same system resistance. Noise emitted from both only shrouded fan and shrouded fan with upstream structures was compared under the same system resistance conditions, and the influences of upstream structures on discrete tonal noise were discussed in detail.

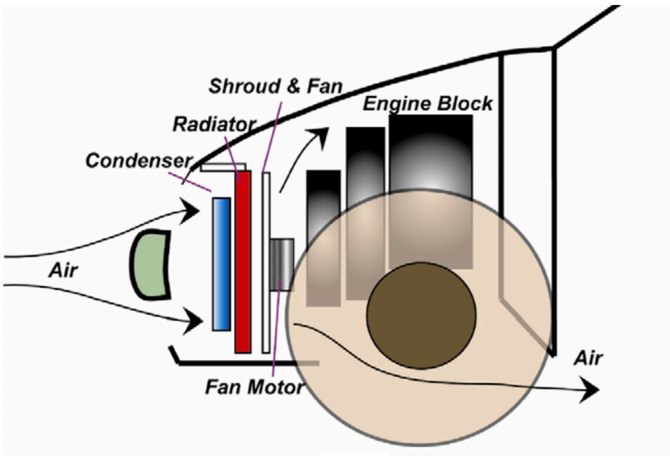

Fig. 1. Schematic configuration of installed axial fan in the engine room of an automobile

2. Experimental setup

2.1 Acoustic fan tester

An acoustic fan tester was designed to measure the performance and noise of the axial fan under various actual operating conditions. Fig. 2 shows a schematic of the facilities for measuring the performance and noise, consisting of an anechoic chamber, an acoustic fan tester, and a silent suction system. An acoustic fan tester with dimensions 1 (W) × 1 (H) × 2.4 (L) m was installed in an anechoic chamber with dimensions of 6 (W) × 4 (H) × 5 (L) m to attenuate the influences of the background and reflected noise efficiently. The experimental facilities were designed and constructed in accordance with the AMCA 210-99 standard [30]. An AMCA standard nozzle with a long radius was adopted to easily calculate the volume flow rate of the fan from the measured differential pressure (ΔP_{nozzle}). Flow settling screens were installed at the front and rear of the flow nozzle to provide uniform flow patterns. Screens of square mesh made of round wire with an open area of 56% were selected. In this study, the grille and front fascia are neglected, and the downstream engine blocks are modeled by a damper. In practice, the downstream engine blocks can raise the system resistance of the internal chamber across the fan assembly, which has a direct impact on the resulting air flow rate. The damper was installed at the end of the chamber to control the downstream air flow and the system resistance using throttle control and a blower. A silent suction system was constructed outside the anechoic chamber to allow air flow rates to pass through the fan and into the acoustic fan tester.

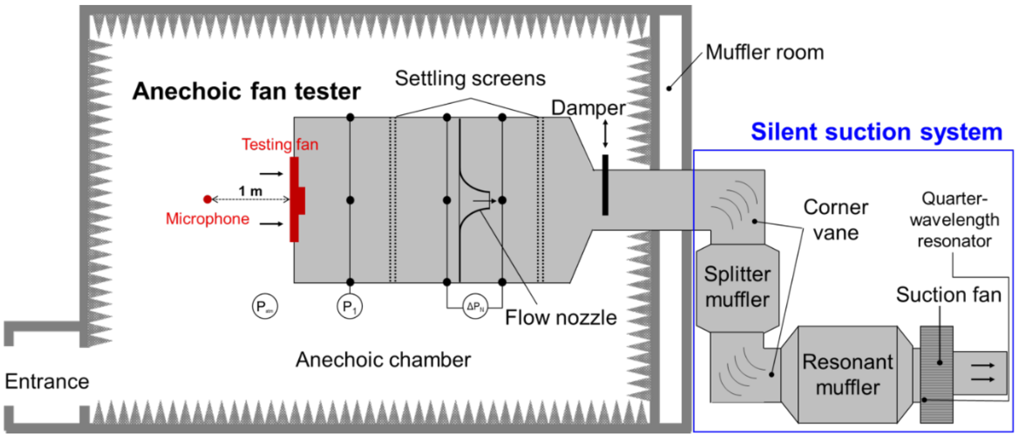

Fig. 2. Schematic of the acoustic fan tester with silent suction system

2.2 Measuring equipment

The experimental setup for measuring the performance and noise of the axial fan system and the apparatus for acquiring the data are shown in Figs. 3 and 4, respectively. The rotational speed of the fan mounted on the electric motor is controlled by the current and voltage values supplied from a DC power supply (UP-3050, 30V-50A). The rotational speed of the fan is measured using a tachometer (UT-372). For the measurement of the fan performance, the static pressure (ΔP_s) is measured with a pressure scanner (DSA-3217) connected to the ring of the four pressure taps located at the center of each of the four plenum walls. The sampling rates of the pressure scanner is up to 0.5 kHz/channel with a long-term system accuracy of ±0.05% full scale. The pressure data of 5,000 values are averaged for 10 s to measure the steady value of the pressure. In addition, the air flow rate passing through the fan is measured by a standard nozzle using a unique relationship between the nozzle discharge coefficient and its Reynolds number in accordance with the standard of AMCA 210-99 [30]. Half-inch free-field microphones of Brüel & Kjær (B&K) 4190 are used to measure the acoustic pressure radiated from the fan. The microphone is installed in front of the center of the fan, and the distance between the microphone and the fan is 1 m, in accordance with ISO 7779 standards, as shown in Fig. 3. The microphones have a nominal sensitivity of 50 $mVPa^{-1}$, a dynamic range of 14.6–146 dB, and a flat frequency response of up to 20 kHz. The microphones are used in conjunction with a B&K Nexus 2690 amplifier, and their sensitivity is validated using a B&K model 4231 sound calibrator. The microphone outputs are acquired using an NI DAQ-4431 24-bit digitizer. The measured sound pressure levels (SPLs) at the standard measuring point are averaged for 100 s to eliminate unexpected noise and capture repeated fan noise.

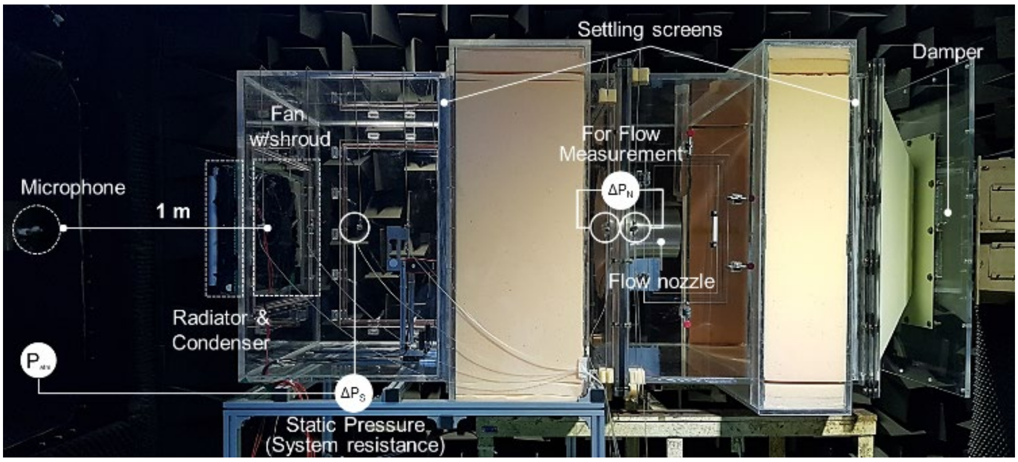

Fig. 3. Experimental setup for inflow effect using the acoustic fan tester

Fig. 4. Data collection apparatus of the fan performance data and sound pressure signal

2.3 P-Q curve and background noise

A performance characteristics diagram of the fans, known as the P-Q curve, shows the relationship between the air flow rate and static pressure. Here, the air flow rate indicates the total amount of air passing through the fan per unit time, and the static pressure is the pressure difference between the inlet and outlet of the fan. The inlet pressure (p_1) is considered as the pressure at the position in front of the fan, while the outlet pressure (p_2) is measured behind the fan. When the axial fan operates under the free field condition where there is no upstream structure, the inlet pressure corresponds to the atmospheric pressure (p_{atm}). The outlet pressure varies owing to the flow impedance caused by the structures behind the fan system. The static pressure is the system resistance that determines the amount of air passing through the fan. The fan can provide the maximum airflow rate without any resistance if the static pressure is zero. The air flow rate passing through the fan was measured under various system resistances resulting from the static pressure to verify the measuring capacity of the acoustic fan tester. Fig. 5 shows the fan's P-Q curve measured from the acoustic fan tester, and it was compared with the reference data provided from the Hanon Systems Corporation. On the y-axis, the pressure difference between the inlet and outlet of the axial fan is the measured static pressure, which is the system resistance, and the x-axis indicates the air flow rate induced by the fan. The comparison results show that the measurements obtained by the acoustic fan tester matched well with the reference data [32].

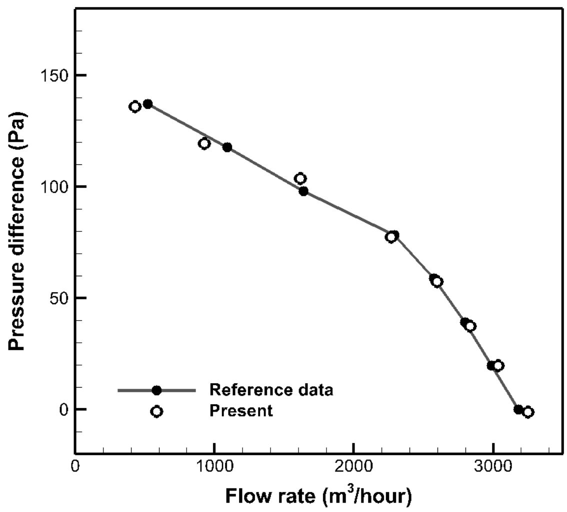

Fig. 5. Comparison of P-Q curve measured by the acoustic fan tester with the reference data

As aforementioned, the acoustic fan tester includes a nozzle for measuring the air flow rate passing through the fan, a damper for controlling the system resistance, and a silent suction system for creating air flow in the fan tester. Because the nozzle, damper, and suction system can generate background noise, the noise level measured from the acoustic fan tester contains background noise emanating from other components as well as the fan noise. The noise generated by the nozzle, damper, and suction system was measured after eliminating all other structures placed in front of the nozzle chamber to investigate the influence of the background noise level. Fig. 6 shows the comparison of the fan noise and background noise with varying air flow rates. Here, the lowest and highest flow rates (denoted as ‘A’ and ‘C’) imply high and zero system resistance conditions, respectively. Moreover, the medium flow rate (denoted as ‘B’) indicates the specific condition in which the lowest fan noise occurs. SPL measurements on the fan are expressed in the A-weighted decibels (dBA) scale, and the range of fan noise varies from 67.7 to 76.2 dBA depending on the system resistances. The comparison results show that the fan noise is at least 13 dB greater than the background noise. This indicates that the fan noise is 20 times greater than the background noise at all operating conditions. Therefore, the aerodynamic noise generated by the rotating fan is much higher than the background noise resulting from the nozzle, damper, and suction system. Furthermore, the acoustic fan tester can be used to measure the fan noise level without interfering with the background noise.

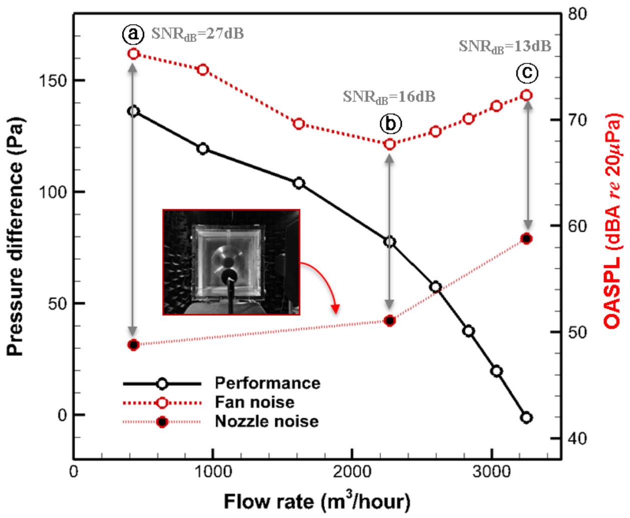

Fig. 6. Comparison of the fan noise and background noise levels with the varying air flow rate

3. Results and discussion

3.1 Fan noise measurement in free-field condition

The automotive cooling system consists of a condenser, radiator, and cooling fan with a shroud. The primary function of the condenser is to exchange heat for an automotive heating, ventilation, and air conditioning (HVAC) system, and the radiator is to remove excessive heat to cool the engine. Because the condenser and radiator are positioned in front of the cooling fan, their existence significantly affects the inflow blowing through the fan; consequently, the inflow variation affects the performance and noise level of the cooling fan system. We examined the impact of the inflow perturbation on the acoustic characteristics of the cooling fan under free field conditions in which there is no system resistance. For this study, three different configurations were considered, depending on the existence of other structures: (a) the fan with the thin shroud (denoted as 'shrouded fan'), (b) the fan with thin shroud and radiator (denoted as 'shrouded fan w/ radiator'), and (c) the fan with thin shroud, radiator, and condenser (denoted as 'shrouded fan w/ radiator and condenser'). The cooling fan is composed of a hub, seven blades, and a band connecting the blades. The diameter of the fan was 394 mm, and its rotational speed was set at 1,700 rpm. The size of the radiator is 610 (L) × 410.5 (H) × 10.8 (W) mm, and that of the condenser is 630 (L) × 382.6 (H) × 12 (W) mm. A microphone (denoted as 'Obz-1') was installed in front of the center of the fan toward the inflow direction at a distance of 1 m, as shown in Fig. 7.

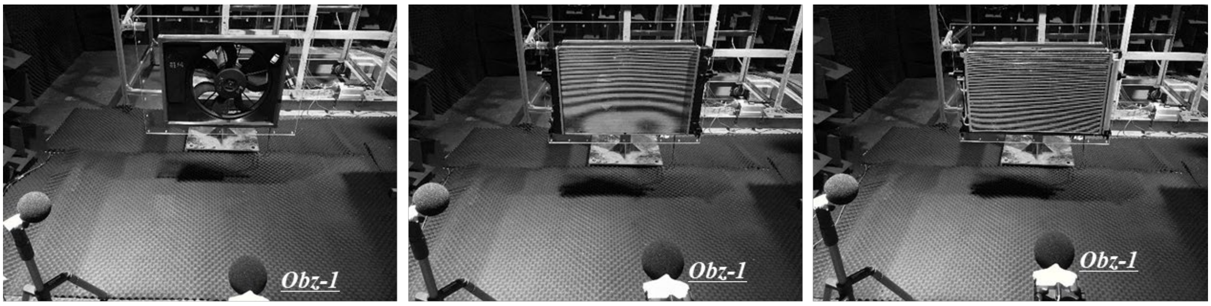

(a) (b) (c)

Fig. 7. Noise measurement of three different configurations in free-field condition: (a) ‘shrouded fan’, (b) ‘shrouded fan w/ radiator’, and (c) ‘shrouded fan w/ radiator and condenser’

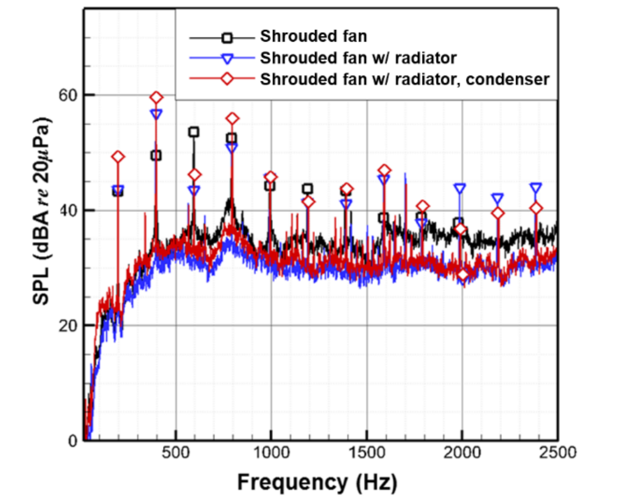

Fig. 8. Comparison of the acoustic spectra of three different configurations in free-field condition

Figure 8 shows the comparison of the acoustic spectra of the three different configurations: ‘shrouded fan’, ‘shrouded fan w/ radiator’, and ‘shrouded fan w/ radiator and condenser’. Note that the results show a significant difference depending on whether the radiator or condenser exists, even if the fans operate at a fixed rotational speed of 1,700 rpm. Tonal noise associated with the BPF of the ‘shrouded fan w/ radiator’ and ‘shrouded fan w/ radiator and condenser’ configurations are higher than that of the ‘shrouded fan’ owing to the inflow effect caused by the existence of other structures. It can be observed that the BPF noise levels of the ‘shrouded fan w/ radiator and condenser’ are approximately 3 to 5 dBA higher than those of the ‘shrouded fan’ and ‘shrouded fan w/radiator’. However, the 3rd and 6th BPF noise levels of the ‘shrouded fan’ are highest, and the broadband noise levels of the ‘shrouded fan w/ radiator’ and ‘shrouded fan w/ radiator and condenser’ are less than those of the ‘shrouded fan’. Further investigations are required to understand this observation. However, the fan performance in terms of the airflow rate and static pressure cannot be assessed at the free-field conditions. Thus, an acoustic fan tester is required to measure the fan performance and noise under the system resistances. In this paper, an experiment using an acoustic fan tester was conducted to investigate the effects of inflow on both the performance and acoustic characteristics of the fan, and our findings are discussed in detail.

3.2 Inflow effects on the fan performance

In the actual operating environment of the automotive axial fan, a radiator and condenser are commonly placed in front of a fan; thus, changing the fan's operating environment, such as system resistance and inflow conditions. Here, we refer to this condition as an inflow effect of the upstream structures. We measured the air flow rate depending on the static pressure using acoustic fan test facilities to investigate the inflow effect on the fan performance. The acoustic fan tester was designed to install the radiator and condenser components along the upstream direction, as shown in Fig. 3. We measured the fan performance of three different configurations: a 'shrouded fan', a 'shrouded fan w/ radiator', and a 'shrouded fan w/ radiator and condenser'. The fan performance can be measured under constant voltage or constant RPM conditions. The constant voltage method measures the fan performance by varying the rotational speed of the fan while maintaining the voltage acting on the electric motor. Meanwhile, the constant RPM method measures the fan performance by varying the voltage produced from the DC power supply while maintaining the rotational speed of the fan. The actual operating environment of automotive cooling fans is a constant voltage condition. However, the rotational speed of the fan should be equal to compare the fan noise under the same performance conditions. Therefore, fan noise data measured under constant RPM conditions were compared.

Figure 9 shows the non-dimensional fan performance curves for three different configurations under constant voltage and RPM conditions. The non-dimensional fan performance curves can be obtained from the calculation of the dimensionless parameters in terms of flow rate and pressure defined as in Eqs. (1) and (2), respectively. Thus, it can be observed that the two methods of measuring fan performance yield similar results by using non-dimensional fan performance curves, although the rotational speeds of the fan are different. The cooling fan systems are often exposed to different inflow conditions depending on the existence of other structures in front of the shrouded fan. As shown in Fig. 9, we obtained different P-Q diagrams presented in a non-dimensional form, although the same fan was used for the measurements. This indicates that the inflow effect caused by upstream structures has a significant effect on the performance of a fan. In the case of the existence of upstream structures, such as the radiator or condenser, the air flow rate passing through the cooling fan systems decreases at the same static pressure conditions compared to the shrouded fan configuration. It can be observed that the measured static pressure is changed depending on whether the structures exist in front of the fan. It indicates that the fans are subjected to different system resistance conditions, although they operate at the same rotational speed. Therefore, the static pressure measured from the different shroud fan configurations should be corrected to compare their SPLs under the same systems resistance condition. In this paper, the static pressure correction method was proposed to compare the fan noise characteristics of the three configurations under the same system resistance and investigate the inflow effects caused by the upstream structures on the tonal noise.

$$\phi = \frac{Q}{N_{rps} d_{fan}^3} \qquad \text{Eq. (1)}$$

$$\psi = \frac{\Delta p_s}{\rho N_{rps}^2 d_{fan}^2} \qquad \text{Eq. (2)}$$

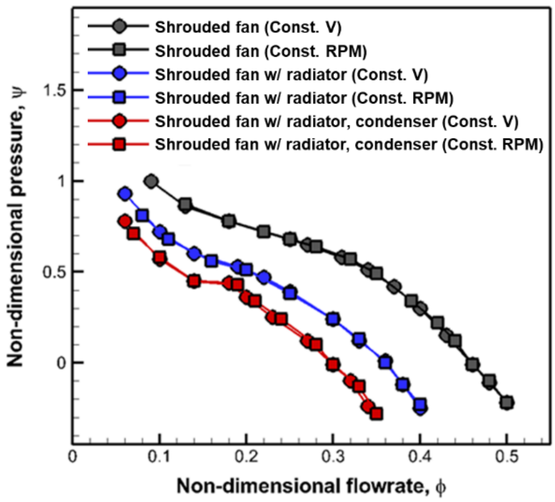

Fig. 9. Comparison of non-dimensional performance curves for three different fan systems: 'shrouded fan', 'shrouded fan w/ radiator', 'shrouded fan w/ radiator and condenser'

3.3 Static pressure correction method

The air flow rate and noise measurements should be compared under the same system resistance conditions to investigate the inflow effects resulting from the radiator or condenser on the fan performance and SPLs. Because our measurements of the static pressure (ΔP_s) for the cases of both 'shrouded fan w/ radiator' and 'shrouded fan w/ radiator and condenser' include the amount of the pressure drop (ΔP_{drop}), they should be corrected to ensure that the performance and noise of the three different configurations are compared under the same conditions. This can be achieved by compensating for the pressure drop from the measured static pressure.

We analyzed how the measured static pressure changes depending on whether the upstream structures exist. Fig. 10 shows the relationship between the static pressure, system resistance, and pressure drop caused by upstream structures, including the radiator and condenser. The pressure difference between the inlet and outlet of the fan is the static pressure, as shown in Eq. (3), where p_1 and p_2 are the inlet and outlet pressures, respectively. As shown in Fig. 10(a), for the shrouded fan only, the inlet pressure is the atmospheric pressure (p_{atm}), as shown in Eq. (4).

$$\Delta p_s = p_2 - p_1 \qquad \text{Eq. (3)}$$

$$p_1 = p_{atm} \qquad \text{Eq. (4)}$$

However, if the upstream structures are placed in front of the shrouded fan, as shown in Figs. 10 (b) and (c), an additional pressure drop occurs, and the fan inlet pressure changes as in Eq. (5). Thus, the fans are subjected to different system resistance conditions. The amount of pressure drop caused by the radiator or condenser should be considered to correct the inlet pressure.

$$p_1 = p_{atm} - p_{drop} \qquad \text{Eq. (5)}$$

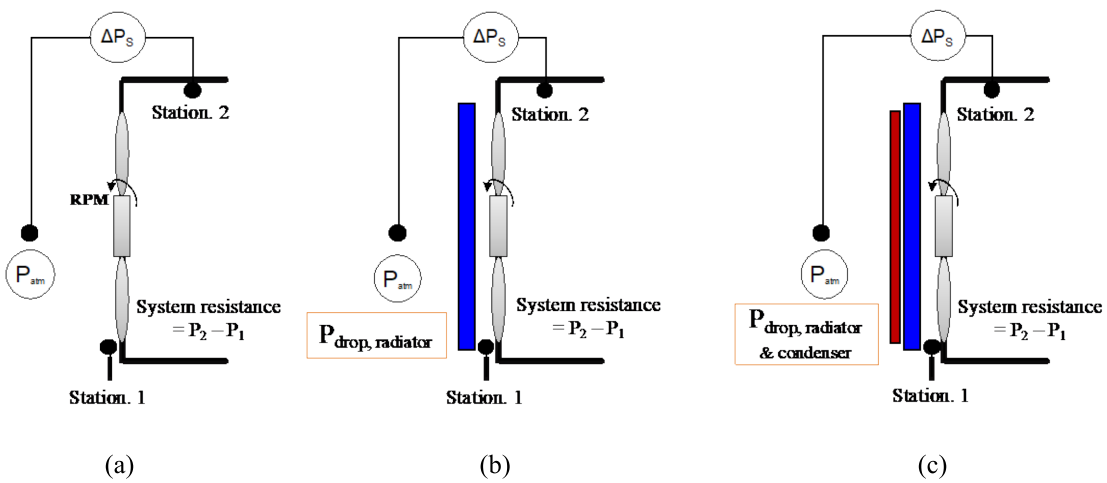

Fig. 10. Measurements of the static pressure for three different fan systems: (a) ‘shrouded fan’, (b) ‘shrouded fan w/ radiator’, (c) ‘shrouded fan w/ radiator and condenser’

The pressure drop (ΔP_{drop}) includes air leakage from the geometric gap between the shrouded fan, radiator, and condenser, and the drag caused by airflow blowing through the radiator or condenser. Here, we can measure the amount of pressure drop that occurs due to a radiator or condenser using an acoustic fan tester. The pressure drops for the three configurations were measured under various air flow rates induced by the suction fan of the acoustic fan tester after removing the fan blade from the acoustic fan tester, as shown in Fig. 11(a). After that, the measured pressure drop of the shrouded fan with upstream structures was subtracted from that of the shrouded fan to evaluate the amount of the pressure drop owing to the radiator or condenser. Fig. 11(b) illustrates the variations of the measured pressure drop resulting from the radiator and condenser, and trends can be modeled as a function of inflow rates. Consequently, the static pressure correction method provides an empirical function to compensate for the pressure drop in each upstream structure according to various air flow rates.

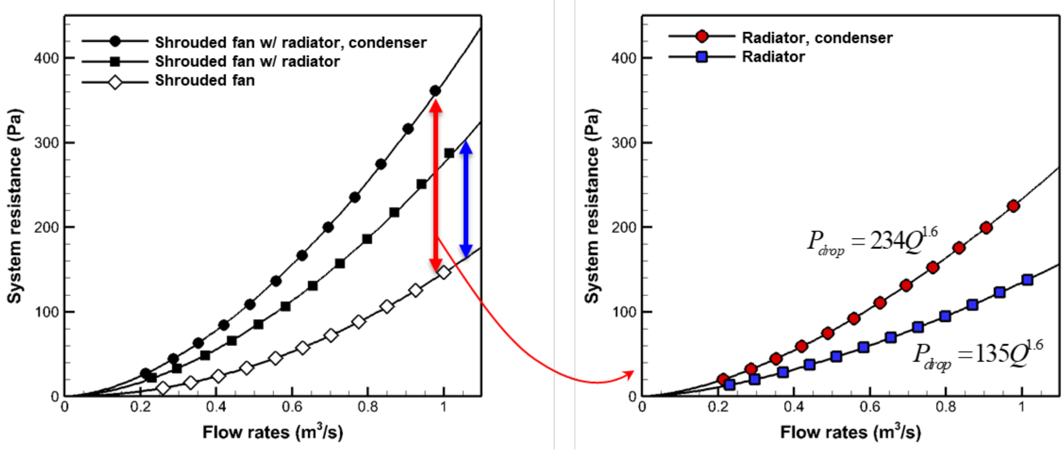

(a) (b)

Fig. 11. Performance correction for inflow effect using system resistance of cooling subsystem; (a) System resistance, (b) Empirical correction function

The corrected static pressure can be obtained by compensating for the amount of pressure drop calculated from the empirical correction function, and the corrected non-dimensional pressure can be evaluated using Eqs. (6) and (7). The corrected non-dimensional performance curves are presented in Fig. 12. It can be observed that the corrected non-dimensional performance curves for the three types of cooling system configurations are practically drawn as one characteristic curve at above 0.16 of non-dimensional air flow rates. The performance characteristic curves of the three configurations do not match a single curve, even when applying inflow effect correction at a non-dimensional air flow rate below 0.16. Thus, the fan blades enter the stall region in other studies [33−35]. Based on these results, the stall region of the fan blades can be identified from the performance curves.

$$\Delta p_{s,correction} = \Delta p_s + p_{drop} \qquad \text{Eq. (6)}$$

$$\psi_{correction} = \frac{\Delta p_{s,correction}}{\rho N_{rps}^2 d_{fan}^2} \qquad \text{Eq. (7)}$$

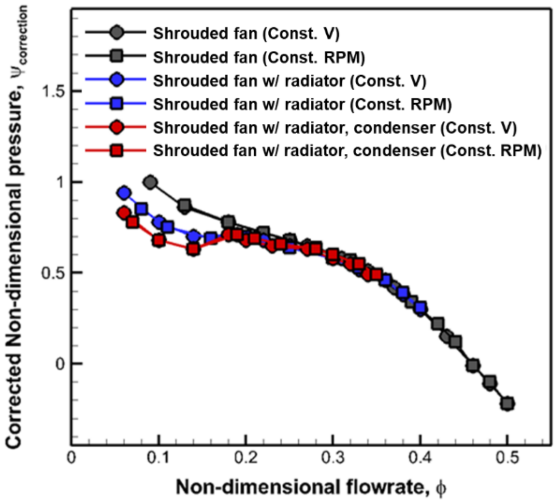

Fig. 12. Corrected non-dimensional P-Q curve at constant voltage and rpm conditions

3.4 Inflow effects on the tonal noise

In the previous section, the measured static pressure was compensated by introducing the inflow correction method to compare the fan noise characteristics of the three configurations for the cooling subsystems at the same system resistance. Thus, we can compare the noise under the same conditions. As noted above, the operating conditions of the fan were measured by maintaining a constant rotational speed to compare the fan noise characteristics for the rotational frequencies. Fig. 13(a) depicts the overall sound pressure level (SPL) for the three configurations at each performance based on the constant rotational speed (1700rpm) of the fan. The trends of the noise characteristics of the 'shrouded fan w/ radiator' and 'shrouded fan w/ radiator and condenser' are almost similar to those of the noise characteristics of the shrouded fan at each performance. The nomenclatures ('A', 'B' and 'C' of the regions) were reused to represent the performance regions (flow rates and static pressure), as noted in Section 2.3. At region 'A', if high static pressure (high system resistance) and low flow rate induced by the cooling fan exist, it can be inferred that its blades enter the stall region. In particular, at region 'A', which is below

0.16 of non-dimensional air flow rate, the corrected non-dimensional static pressure of the ‘shrouded fan’, ‘shrouded fan w/ radiator’, and ‘shrouded fan w/ radiator and condenser’ are not consistent. Therefore, the linear correction for upstream system resistance does not fit well because most of the fan blades enter the rotating stall [18, 19]. In addition, the broadband noise emitted by mature stall cells on the blades is more dominant than tonal noise. The results obtained by the acoustic fan tester are in good agreement with the NASA Glenn Research Center [36] and Hodgson et al. [17] in accordance with ISO 10302; they found that the emission of a broadband noise of the fan increases under high system resistance. In addition, the broadband noise is emitted by strong tip-leakage flow caused by high system resistance [20]. Based on the results of previous researchers [9, 13, 17, 20, 33−35], it can be anticipated that broadband noise is the dominant noise source at region ‘A’. As aforementioned, the performance mismatch for all configurations can be observed due to the onset of the blade stall, even though the static pressure corrected by the upstream structures has been conducted. At region ‘B’, as ideal performance, such as medium static pressure and medium air flow rates, the cooling systems of all of the configurations have the lowest noise level. At region ‘C’, the static pressure decreases, and then the air flow rate induced by the cooling fan increases. Therefore, it can be estimated that fan noise increases owing to an increase in air flow rates. In the region between ‘A’ and ‘B’, the overall SPL of the ‘shrouded fan w/ radiator’ and ‘shrouded fan w/ radiator and condenser’ are almost the same. Conversely, the overall SPL of the ‘shrouded fan w/ radiator’ is lower than that of the ‘shrouded fan w/ radiator and condenser’ at the region between ‘B’ and ‘C’. Moreover, the ‘shrouded fan w/ radiator and condenser’ has the highest noise level at region ‘C’, even though the ‘shrouded fan’ has the highest noise level at most performance ranges. Therefore, the noise level of the measurement position is reduced at most performance ranges except in region ‘C’ owing to the upstream structures.

The overall SPL can be divided into a broadband component and a blade passing frequency (BPF) component for a detailed analysis of the noise characteristics, as shown in Fig. 13(b). At all performance ranges, it can be observed that the broadband noise of the ‘shrouded fan’ is higher than that of the other configurations. However, different results can be obtained regarding the tonal noise according to upstream structures at between regions ‘B and ‘C’. Specifically, at region ‘C’, the tonal noise of the ‘shrouded fan w/ radiator and condenser’ significantly increases as the air flow rates increase. In the following order, the tonal noise of the ‘shrouded fan w/ radiator’ increased more than that of the ‘shrouded fan’. Note that the upstream structure significantly changes the tonal noise as the air flow rates increase, even though the configurations have similar fan performance.

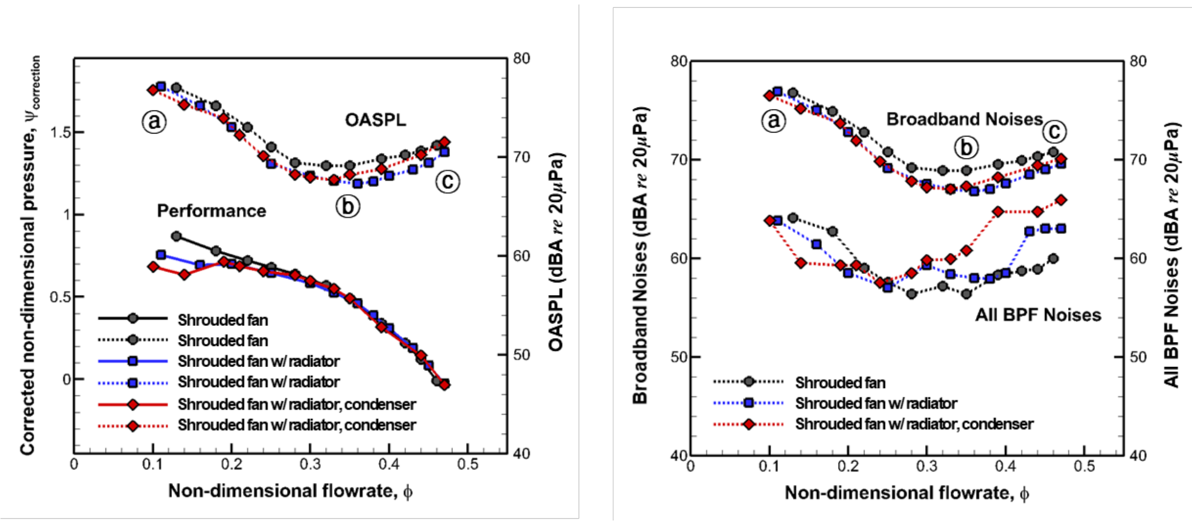

(a) (b)

Fig. 13. Inflow effects on acoustic characteristics: (a) Overall SPL and (b) tonal and broadband noises

Figure 14 shows the comparison of the acoustic spectra of the 'shrouded fan', 'shrouded fan w/ radiator', and 'shrouded fan w/ radiator and condenser' at each performance regions: 'A', 'B' and 'C'. At region 'A', the trends of spectra of the 'shrouded fan w/ radiator' and 'shrouded fan w/ radiator and condenser' are the same as the result of the 'shrouded fan' owing to the onset of stall. Under rotating stall conditions, the characteristic of the tonal and broadband noises of the shrouded fan is similar to the numerical research by Zhang [27, 28]. Owing to the onset of the rotating stall, it can be observed that the noise characteristics of other configurations for upstream structures are similar to that of the shrouded fan. In other performance regions, 'B' and 'C', it can be observed that the characteristics of tonal noise have changed by upstream structures. At region 'B', the tonal noise level of the 'shrouded fan w/ radiator' and 'shrouded fan w/ radiator and condenser' are higher than that of the 'shrouded fan'. This phenomenon increases in region 'C' where the flow rate increases. In addition, the tonal noise level of the 'shrouded fan w/ radiator and condenser' is higher than that of the 'shrouded fan w/ radiator'. Simply, it can be inferred that the more upstream structures, the more tonal noise increases. In particular, the tonal noise level of the 1st and 2nd BPF components of the 'shrouded fan w/ radiator', and 'shrouded fan w/ radiator and condenser' are higher than that of the 'shrouded fan' at regions 'B' and 'C'. Conversely, the tonal noise level of the 3rd and 4th BPF components of the 'shrouded fan w/ radiator' is less than that of the 'shrouded fan' at regions 'B' and 'C'. Tonal noise level of the 4th BPF components of the 'shrouded fan w/ radiator and condenser' is higher than that of the 'shrouded fan'. The tonal noise level of the 1st to 4th BPF components of the 'shrouded fan w/ radiator and condenser' is higher than that of the 'shrouded fan w/ radiator'. Non-uniform inflow caused by upstream structures, induces periodical pressure on the surface of the fan blades [23−25]. In addition, as the flow rate increases from region 'B' to 'C', it can be observed that the non-uniform inflow causes the tonal noises to increase, especially the noise level of the 1st to 4th BPF components of the 'shrouded fan w/ radiator and condenser' significantly increased compared to that of other configurations. Tonal noise emitted from the rotating fan blade is generated due to displacement of fluid by the rotor blade and the aerodynamic force exerted on the fluid by the blade surface. Non-uniform inflow cases an asymmetric velocity distribution on the fan blade and an increase in the turbulence intensity. The fan blade experiences the unsteady and azimuthal variation in the aerodynamic loads that give rise to a significantly larger radiated tonal noise, particularly the dipole noise component, compared to the tonal noise generated by a uniform flow [37]. Chandrashekar [38] has theoretically demonstrated that tonal noise increases by about 6 dB as the turbulence intensity increases from 1% to 2% when placing the upstream structure in front of the rotor. However, the inflow effect by upstream structures is not affected at higher system resistance (region 'A') owing to the rotating stall phenomenon.

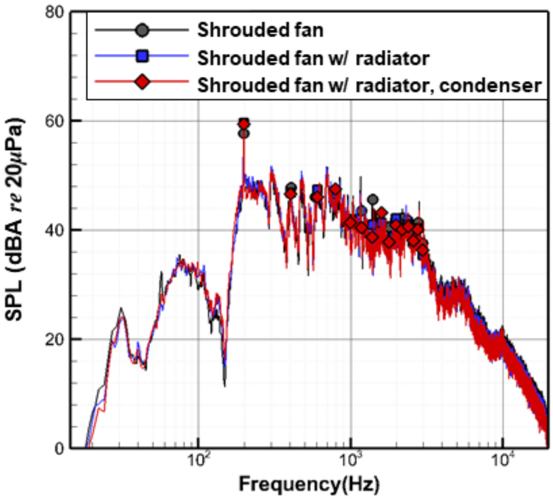

(a)

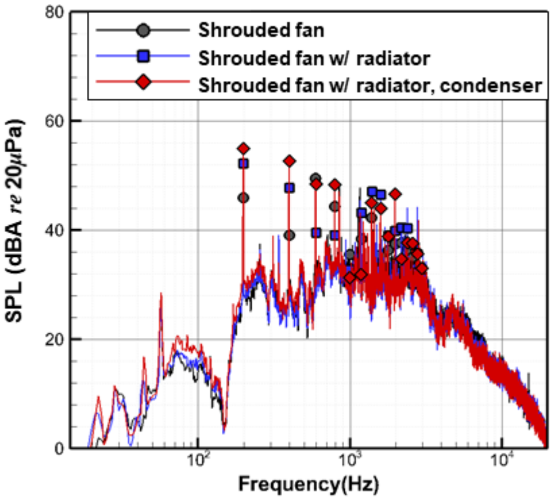

(b)

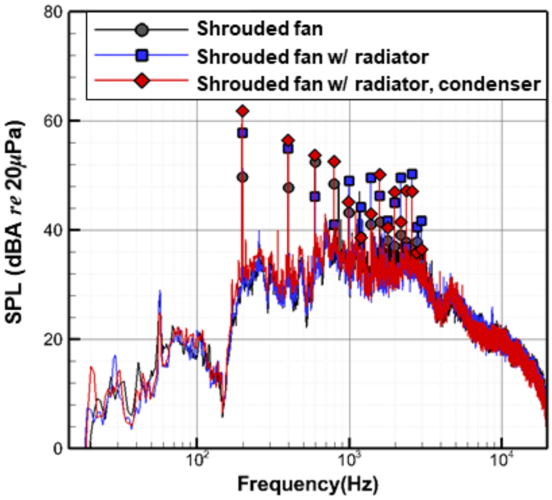

(c)

Fig. 14. Inflow effects on the acoustic spectra: (a) higher system resistance (region 'A'), (b) medium system resistance (region 'B'), (c) zero system resistance (region 'C')

Figure 15 depicts broadband noise spectra of three configurations at zero system resistance (region 'C') conditions. It can be seen that the broadband noise spectra of 'shrouded fan' are approximately 2~3 dBA larger than those of 'shrouded fan w/ radiator' and 'shrouded fan w/ radiator, condenser' in the frequency range of 1 to 3 kHz. In the author's previous paper [39], it was found that one of the dominant broadband noise sources of 'shrouded fan' is the turbulent flow interaction between the serrated shroud and recirculating flow. Piellard and Couty [40] demonstrated that the stationary acoustic ring located in front of the axial fan (along the upstream direction) helps to prevent the generation of the recirculation flow near the blade tip and the onset of the flow interaction, thus leading to 2.5 dBA reduction of broadband noise. It can be inferred that the existence of the upstream structures can contribute to reducing the level of broadband noise of the axial fan system. This possibility will be investigated in future work because the scope of the current work is to study the inflow effects on tonal noise.

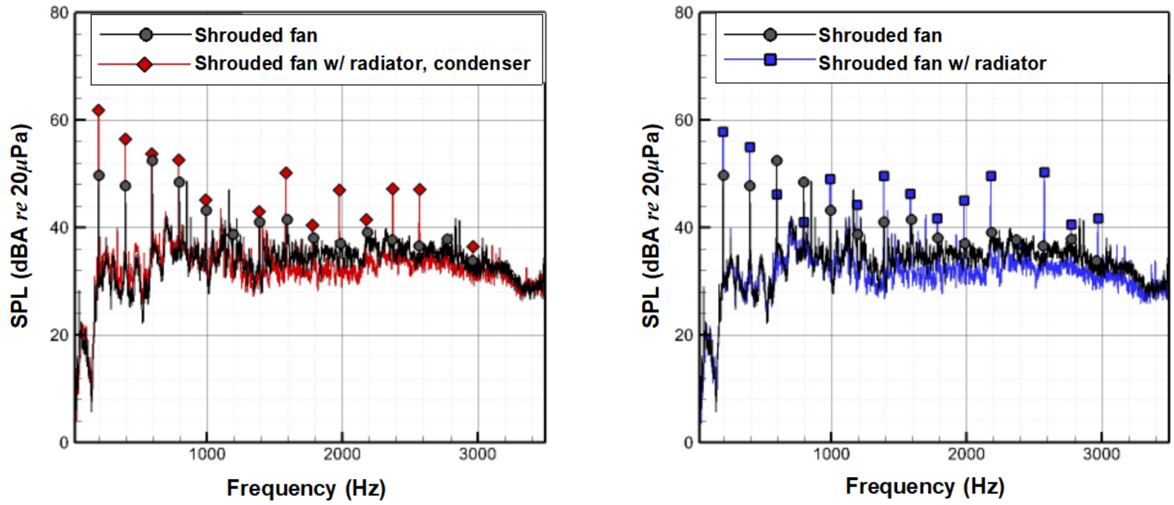

(a) (b)

Fig. 15. Broadband noise spectra of three different configurations at zero system resistance (region 'C'): (a) comparison of 'shrouded fan' and 'shrouded fan w/ radiator and condenser', (b) comparison of 'shrouded fan' and 'shrouded fan w/ radiator'

4. Conclusion

Automotive cooling fans operate with the upstream structures located in the front of them under the actual operational environment. These structures induce the inflow effect that affects the inflow velocity distribution and inlet pressure. In this study, three shrouded fan configurations, including 'shrouded fan', 'shrouded fan w/ radiator', and 'shrouded fan w/ radiator and condenser', were considered to investigate the inflow effects caused by the upstream structures on the performance and noise characteristics of the fans. An acoustic fan tester installed in an anechoic chamber facility with the silent suction system was designed to simultaneously measure the air flow rate, static pressure, and sound pressure levels of the shrouded fan configurations. In addition, the static pressure correction method was proposed to adjust for the changing measured static pressure owing to the upstream structures. This correction method provided an empirical function to compensate for the amount of the pressure drop induced by each upstream structure, and the fans were subjected to the same system resistance conditions. Results showed that the tonal noise levels of the shrouded fan with the upstream structures increased owing to non-uniform inflow distribution compared to those of the shrouded fan configuration for all the conditions except for the low inflow rate conditions where the blade stall occurs. In addition, the tonal noise levels of the 'shrouded fan w/ radiator and condenser' were much higher than other configurations, particularly the tonal noise levels associated with 1st to 4th BPF components increased significantly. However, broadband noise in the frequency range of 1 to 3 kHz decreased when the upstream structures, such as radiator and condenser, were installed in front of the axial fan since they could help to prevent the generation of the recirculation flow near the blade tip and the onset of the flow interaction

The acoustic fan tester installed in the anechoic chamber is useful to examine the aerodynamic performance and noise levels of the axial fans. The measurements in this facility can consider the actual operating environment, from low to high system resistance conditions, not free field conditions. The limitation of the current work is that the impacts of the rotational speed on the inflow effect in terms of tonal noise levels were not studied. Future work will examine the sound pressure levels of the axial fan systems with different rotor blades at various rotating speeds and system resistance conditions. Our findings will contribute to the fan blade design and help improve the fan performance and reduce the noise radiated from the rotor blade of the axial fan.

Declaration of competing for interest

The authors declare that they have no known competing financial interests or personal relationships that could have appeared to influence the work reported in this paper.

Acknowledgments

This study was supported by the National Research Foundation of Korea (NRF) grant funded by the Ministry of Science, ICT & Future Planning (NRF-2017-R1A5A1015311, 2020R1I1A1A01066929, and 2021R1C1C1010198).

References

[1] Wang Y, Gao Q, Zhang T, Wang G, Jiang Z, Li Y. Advances in Integrated Vehicle Thermal Management and Numerical Simulation. Energies 2017;10(10):1636.

[2] Li B, Kuo H, Wang X, Chen Y, Wang Y, Gerada D, Worall S, Stone I, Yan Y. Thermal Management of Electrified Propulsion System for Low-Carbon Vehicles. Automotive Innovation 2020;3:299–316.

[3] Ouis D. Annoyance from road traffic noise: a review. J Environ Psychol 2001;21(1):101–120.

[4] Jafari S, Dunne JF, Langari M, Yang Z, Pirault JP, Long CA, Jose JT. A review of evaporative cooling system concepts for engine thermal management in motor vehicles. Proceedings of the Institution of Mechanical Engineers, Part D: Journal of Automobile Engineering 2017;231(8):1126–1143.

[5] Deulgaonkar VR, Kallurkar SP, Mattani AG. Review and diagnostics of noise and vibrations in automobiles. International Journal of Modern Engineering Research 2011;1(2):242–246.

[6] Pang SC, Kalam MA, Masjuki HH, Hazrat MA. A review on air flow and coolant flow circuit in vehicles' cooling system. Int J Heat Mass Transf 2012;55:6295–6306.

[7] Kim HJ, Kim CJ. A numerical analysis for the cooling module related to automobile air-conditioning system. Appl Therm Eng 2008;28:1896–1905.

[8] ISO 1680:2013. Acoustics–Test code for the measurement of airborne noise emitted by rotating electrical machines; 2013.

[9] Bolton AN. Installation Effects in Fan Systems. Proceedings of the Institution of Mechanical Engineers, Part A: Journal of Power and Energy 1990; 204(3):201–21.

[10] Longhouse RE. Control of tip-vortex noise of axial flow fans by rotating shrouds. J Sound Vib 1978;58(2):201–214.

[11] Maling Jr GC. Historical developments in the control of noise generated by small air-moving devices. J Acoust Soc Am 1994;96:3237.

[12] Fukan T, Jang CM. Tip clearance noise of axial flow fans operating at design and off-design condition. J Sound Vib 2004;275:1027–1050.

[13] Stephens DB, Morris SC. A method for quantifying the acoustic transfer function of a ducted rotor. J Sound Vib 2008;313:97–112.

[15] Heo S, Ha M, Kim TH, Heo CC. Development of high-performance and low-noise axial-flow fan units in their local operating region. J Mech Sci Technol 2015;29:3653–3662.

[16] Schmitt JG, Nelson DA, Phillips J. An automated system for the acoustical and aerodynamic characterization of small air moving devices. J Acoust Soc Am 2005;118:1978.

[17] Hodgson M. Isabella L. Experimental study of the noise emission of personal computer cooling fans. Appl Acoust 2006;67(9):849–863.

[18] Čudina M, Prezelj J. Noise generation by vacuum cleaner suction units. Part III. Contribution of structure-borne noise to total sound pressure level. Appl Acoust 2007;68(5):521–537.

[19] MacDonald MA, Gullbrand J, Nishic Y, Baughd E. Notebook blower inlet flow and acoustics: Experiments and simulations. Noise Control Eng J 2009;57(4): 348–359.

[20] Canepa E, Cattanei A, Zecchin FM, Milanese G, Parodi D. An experimental investigation on the tip leakage noise in axial-flow fans with rotating shroud. J Sound Vib 2016;375:115–131.

[21] Lin SC, Chou CA. Blockage effect of axial-flow fans applied on heat sink assembly. Appl Therm Eng 2004;24:2375–2389.

[22] Suzuki A, Soya A. Study on the fan noise reduction for automotive radiator cooling fans. SAE Technical Paper 2005-01-0601; 2005.

[23] Gérard A, Berry A, Masson P, Gervais Y. Experimental validation of tonal noise control from subsonic axial fans using flow control obstructions J Sound Vib 2009;321(1-2):8–25.

[24] Gérard A, Berry A, Masson P, Gervais Y. Modelling of tonal noise control from subsonic axial fans using flow control obstructions. J Sound Vib 2009;321(1-2):26–44.

[25] Sturm M, Carolus T. Tonal fan noise of an isolated axial fan rotor due to inhomogeneous coherent structures at the intake. Noise Control Eng J 2012;60(6):699–706.

[26] Rynell A, Efraimsson G, Chevalier M, Abom M. Acoustic characteristics of a heavy duty vehicle cooling module. Appl Acoust 2016;111:67–76.

[27] Rynell A, Chevalier M, Åbom M, Efraimsson G. A numerical study of noise characteristics originating from a shrouded subsonic automotive fan. Appl Acoust 2018;140:110–121.

[28] Pérot F, Kim MS, Moreau S, Henner M. Axial fan noise aeroacoustics predictions and inflow effect on tonal noise using LBM. CFD Canada 2013 Conference, Canada; 2013.

[29] Park M, Jang J, Lee DJ. Noise prediction of ducted fan unmanned aerial vehicles considering strut effect in hover. Int J Aeronaut Space Sci 2017;18(1):144–153.

[30] Standard AMCA, 210-99: Laboratory Methods of Testing Fans for Aerodynamic Performance Rating, Air Movement and Control Association International, Inc,; 1999.

[31] ISO 5801:2007. Industrial fans–Performance testing using standardized airways; 2007.

[32] Jung W, Song S, Park M, Lee D. The Noise Prediction of Automotive Axial Fan with Different Blade Sweep Angle Using Unsteady CFD Analysis. In Proceedings of Fan 2015 International Conference; 2015

[33] Čudina M. Noise generation in vane axial fans due to rotating stall and surge. Proceedings of the Institution of Mechanical Engineers, Part C: Journal of Mechanical Engineering Science 2001;215(1):57–64.

[34] Zhang L, Wang R, Wang S. Simulation of broadband noise sources of an axial fan under rotating stall conditions. Advances in Mechanical Engineering 2015;2014:507079.

[35] Zhang L, Yan C, He R, Li K, Zhang Q. Numerical Study on the Acoustic Characteristics of an Axial Fan under Rotating Stall Condition. Energies 2017;10(12):1945.

[36] Koch LD, Van Zante DE, Wernet MP, Podboy GG. An Assessment of NASA Glenn's Aeroacoustic Experimental and Predictive Capabilities for Installed Cooling Fans; Part 2: Source Identification and Validation. NASA/TM—2006-214450; 2006.

[37] Gérard A, Berry A, Masson P, Gervais Y. Experimental validation of tonal noise control from subsonic axial fans using flow control obstructions. J Sound Vib 2009; 321(1-2): 8–25.

[38] Chandrashekhara N. Tone radiation from axial flow fans running in turbulent flow. J Sound Vib 1971;18(4): 533–543.

[39] Park M, Lee DJ. Sources of broadband noise of an automotive cooling fan. Appl Acoust 2017;118:66–75.

[40] Piellard M, Coutty BB, Le Goff V, Vidal V, Pérot F. Direct aeroacoustics simulation of automotive engine cooling fan system: effect of upstream geometry on broadband noise. In 20th AIAA/CEAS Aeroacoustics Conference. 2014.